Autonomous Formation-Flying Sensor for the StarLight Mission

M. Aung,[1] G. H. Purcell,[2] J. Y. Tien,[2] L. E. Young,[2] L. R. Amaro,[3] J. Srinivasan,[2]
M. A. Ciminera,[4] and Y. J. Chong[2]

A formation-flying sensor that can determine spacecraft separation with a maximum uncertainty of 2 cm, measure the bearing angles of the remote spacecraft with a maximum uncertainty of a minute of arc, and operate with a wide field of view autonomously in deep space has been designed and prototyped. It is the autonomous formation-flying (AFF) sensor that operates at 32 GHz (Ka-band) using technology similar to that of the Global Positioning System (GPS). A significant challenge lies in the simultaneous requirements for precision and a wide field of view, mandating a substantial technology development effort and design of a sensor with some novel features. Through development of a prototype, the AFF sensor has been extensively characterized and the key technology risks have been retired. It has been concluded that the AFF sensor can meet the (2-cm, 1-arcmin) requirement within the StarLight two-spacecraft stellar optical interferometer mission. An overview of the sensor design, results of the technology development, conclusions of the technology investigations, and highlights of the related inter-spacecraft issues are presented in this article.

I. Introduction

The StarLight mission, an element of NASA's Origins Program, was designed for the first-time demonstration of two technologies: stellar optical interferometry on multiple spacecraft and autonomous, precise formation flying of multiple spacecraft [5].[5] These technologies will apply to future missions such as the Terrestrial Planet Finder (TPF), Planet Imager, Micro-Arcsecond X-ray Imaging Mission (MAXIM), and other deep-space missions requiring autonomous, precise formation flying to enable a distributed instrument to operate cooperatively across multiple spacecraft.

---

[1] Autonomy and Control Section.

[2] Tracking Systems and Applications Section.

[3] Spacecraft Telecommunications Equipment Section.

[4] Communications Ground Systems Section.

[5] In February 2002, NASA terminated the flight portion of the StarLight mission. At that time, the Terrestrial Planet Finder (TPF) technology program adopted portions of the StarLight technology work applicable to the TPF mission. The autonomous formation-flying (AFF) sensor technology work was adopted. In this article, the AFF sensor is presented within the StarLight context. The AFF sensor technology will be carried forward to the TPF design.

The research described in this publication was carried out by the Jet Propulsion Laboratory, California Institute of Technology, under a contract with the National Aeronautics and Space Administration.

The StarLight mission is composed of two spacecraft, the collector spacecraft and the combiner spacecraft (see Fig. 1). After initial checkout in a heliocentric, Earth-like orbit, the two spacecraft separate and begin flying in formation at separations between 30 and 1000 meters, without real-time intervention from ground-based mission operations.

Operation of the optical interferometer requires alignment of the two optical paths with sufficient precision for interferometric fringe formation. This alignment is achieved in multiple steps, starting from a lost-in-space condition, where the initial relative range and bearing angles within the post-launch cluster are unknown. In the first step, a radio frequency (RF) system, the autonomous formation-flying (AFF) sensor, enables the formation to be acquired and controlled to an accuracy of ± 10 cm in range and ± 4 arcmin in bearing angle. This accuracy brings the two spacecraft within the search range of the metrology system. The infrared metrology system aligns the combiner boresight with the collector optics, and measures changes in the path length to the 10-nm level of accuracy. Then a siderostat on the collector is adjusted to direct light from the target star to the combiner. The optical alignment is maintained by closed-loop control of the siderostats. Then the delay line in the combiner is varied over as much as 50 mm to find the interferometric fringe. The variable delay line also stabilizes the relative path length of the interfering beams at the nanometer level.

To enable the formation to be initially acquired and controlled to an accuracy of ± 10 cm in range and ± 4 arcmin in bearing angle, a relative sensor is required to provide knowledge of spacecraft separation with a maximum uncertainty of 2 cm and knowledge of the bearing angles of the remote spacecraft with a maximum uncertainty of a minute of arc, and to operate with a wide field of view. For this purpose, an RF sensor, the AFF sensor, was designed [1–4]. It operates at 32 GHz (Ka-band) between a pair of spacecraft, as illustrated for StarLight in Fig. 1.

A significant challenge lies in the simultaneous requirements for precision and a wide field of view, mandating a substantial technology development effort and design of a sensor with some novel features. To retire the key technology risks, a prototype Ka-band AFF sensor was developed to verify the basic algorithms, to validate the complex system distributed over multiple spacecraft, and to assess the end-

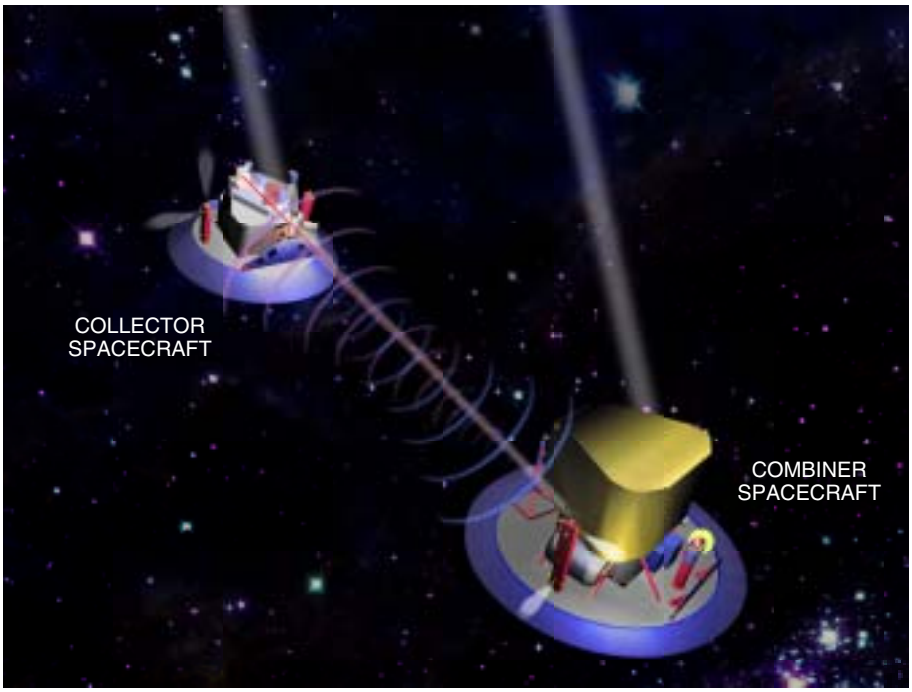

Fig. 1. The AFF sensor within the StarLight mission.

to-end performance in the spacecraft structural environment [6]. The design overview and results of the technology effort are presented in this article.

The requirements also drive a strong interdependence of the AFF sensor design, the spacecraft structural design, the inter-spacecraft acquisition algorithm, and the optical interferometer design. The article also addresses the highlights of these issues.

II. Key Features and Performance Requirements

The AFF sensor is novel in that it performs all of the following functions:

(1) It provides unprecedented accuracy in real-time range (2 cm, 1σ) and bearing-angle (1 arcmin) measurements at spacecraft separation up to 1 km in the "facing" configuration (defined below).

(2) It operates with a nearly 4π-steradian field of view.

(3) It operates autonomously:

   (a) There is no real-time ground-based interaction.

   (b) It is a self-contained instrument, with transmit, receive, and data communication hardware and software for multiple spacecraft.

   (c) It is applicable to deep-space missions. (The Earth-based Global Positioning System (GPS) is not used.)

(4) It generates estimates of range and bearing angles for use in real time by the formation-flying control system.

The AFF sensor range and bearing-angle estimation requirements are listed below and summarized in Table 1. The most stringent requirements apply when the spacecraft directly face each other in the interferometric observation mode. This is when the stellar interferometer acquires the optical signals. The requirements are gradually relaxed for larger off-pointing angles, when the AFF sensor is used to steer the formation into the required geometry. The requirements are specified for three regions:

(1) Facing: angle α between lines of sight and normal to the front side of a spacecraft $\leq$2 deg, both spacecraft.

(2) Nearly facing: 2 deg $< \alpha \leq$ 45 deg for more mispointed spacecraft.

(3) Not facing: 45 deg $< \alpha$ for more mispointed spacecraft.

Table 1. Requirements for AFF sensor performance.

Requirement	Ground calibration and internal measurements			With phase calibration by spacecraft rotation			After bias calibration with laser metrology		
	Facing	Nearly facing	Not facing	Facing	Nearly facing	Not facing	Facing	Nearly facing	Not facing
Range, cm	2	2–30	160	2	2–30	160	2	2–30	160
Range rate, mm/s	1	1	None	1	1	None	1	1	None
Bearing angles, $'$	10	10–900	5400	5	5–600	5400	1	1–600	5400
Bearing rate, $''$/s	10	20	None	10	20	None	10	20	None
Acquisition time, s	300	300	None	300	300	None	300	300	None

III. Design Overview

The AFF sensor is a distributed RF sensor that operates at Ka-band. It is a self-contained system with transmitters and receivers for radio metrics and data transfer on both spacecraft. Each spacecraft will have two transmitting antennas and four receiving antennas:

(1) One transmitting antenna and three receiving antennas on the facing or front side.

(2) One transmitting antenna and one receiving antenna on the back side.

The antennas on the facing side serve to align the spacecraft to the required level. The antennas on the back assist the spacecraft in finding each other in the event they get turned around. This configuration gives near-global coverage.

An AFF sensor on each spacecraft transmits to and receives from the other spacecraft. The signal structure is similar to that used by the GPS:

$$S(t) = A\,P(t)D(t)\cos(2\pi f t + \phi)$$

where

$A =$ signal amplitude

$P(t) =$ ranging code

$D(t) =$ telemetry modulation

$f =$ Ka-band carrier frequency

$\phi =$ carrier phase offset due to range, clock offsets, etc.

The range between the two spacecraft is determined from the delay tracked with the ranging codes. The bearing angles (azimuth, elevation) are determined from the differential carrier phases at the three front-side antennas. The telemetry enables the sensors on each spacecraft to estimate range and bearing.

The transmitters and receivers on the two halves of the sensor on the two spacecraft can transmit and receive simultaneously or operate in a time-division duplexing (TDD) mode, where, on a given spacecraft, the transmission is turned on and off periodically and the receivers process signals only when the transmission is off. Multiple versions of the TDD scheme exist, some requiring time synchronization across spacecraft while others do not.

A. Building Blocks of the AFF Sensor

The AFF sensor is composed of Ka-band antennas, Ka-band transceivers (transmitters and receivers), a frequency and timing subsystem, and a digital baseband processor on each spacecraft. For optimal RF performance of the sensor within the spacecraft structural environment, a Ka-band antenna was designed to maximize the field of view and minimize back-lobe energy. In the transceivers and the frequency and timing subsystem, a complex frequency scheme was designed to facilitate the acquisition of signals and calibration of the sensor distributed over multiple spacecraft. The digital signal processor performs the radio metric processing, signal acquisition, and communication with the AFF sensor on the other spacecraft, as well as general housekeeping functions.

The sensor design and performance interact strongly with the spacecraft design, the interferometer design, and the formation-flying system acquisition design. They are interdependent in terms of accommodation, fields of view, stray light, radio frequency interference, thermal stability, electrical stability, and mechanical stability.

B. Signal Acquisition

After launch and separation of the two spacecraft, the AFF sensors need to acquire the RF carriers, codes, and data of the signals transmitted from the other spacecraft. A proprietary acquisition scheme has been developed to minimize the acquisition time and to allow robust acquisition under low-signal conditions when the antennas are not aligned.

C. Calibration

After signal acquisition on both spacecraft, the sensor needs to be calibrated in the following manner.

1. Rotation Calibration for Initialization. When the receivers on each spacecraft begin to track, the measured phase differences represent a combination of geometry (the desired bearing angles of the remote transmitter) and instrumental offsets, including an integer-cycle ambiguity. As long as the geometry remains fixed, the two contributions are indistinguishable and the bearing angles indeterminate. In order to separate the two components of differenced phase, the spacecraft face one another (using differential range measurements) and perform a series of rotations around the line of sight between them.

2. Antenna Pattern Calibration with Spacecraft Rotations. The antennas' phase patterns will be calibrated prior to launch. However, due to deformations expected at launch, we expect to apply in-flight calibration procedures to achieve the high level of accuracy required by the bearing-angle measurements. The relative phases of pairs of antennas on a spacecraft are calibrated by observing the phase changes as the spacecraft maneuver through bearing-angle changes known from each spacecraft's star camera.

3. Continuous Self-Calibration for Instrumental Variations. Spacecraft thermal, electrical, and mechanical variations introduce instrumental variations that can significantly degrade the sensor performance. Therefore, self-calibration algorithms are employed for continuous internal calibration. Continuous and nearly instantaneous removal of instrumental variations makes the sensor insensitive to thermal and electrical variations.

4. Residual Bias Calibration with Metrology System. After the calibrations listed above, residual biases are removed by comparing the AFF sensor's estimates to the more accurate metrology system's estimates.

IV. Key Technical Challenges

The key technical challenges to be faced in order for the AFF sensor to meet its tight performance requirements while operating with a wide field of view in an autonomous environment include

(1) Adequate RF performance within the spacecraft structure.

(2) Range and bearing-angle estimation in the presence of thermal, electrical, and mechanical instabilities on the spacecraft.

(3) Accommodation on the spacecraft without violation of requirements for the spacecraft subsystems and the interferometer.

(4) Calibration of the distributed system.

(5) Signal acquisition by all receivers.

(6) Operation as a single instrument distributed among multiple spacecraft.

A. RF Performance within the Spacecraft Structure

The spacecraft structure surrounding the antennas creates multipath that modifies their effective patterns. Two major concerns for sensor performance are (1) the isolation between the transmitting antennas and the receiving antennas on the same spacecraft and (2) deviation of the actual antenna patterns from the patterns measured on the ground.

B. Performance in the Presence of Thermal, Electrical, and Mechanical Instabilities

Spacecraft thermal, electrical, and mechanical variations can introduce instrumental variations in the sensor. Because of its stringent performance requirements, even slight variations can significantly degrade the sensor's performance in estimating the range and the bearing angles.

C. Spacecraft Accommodation

In a formation-flying interferometer mission, the RF sensors and the optical instruments need to be accommodated and operated harmoniously within the spacecraft. The AFF sensor radiates and receives in the same hemisphere as the metrology and starlight paths, and conflicting requirements result. An example is the AFF antennas. Ideally, the antennas are made of reflective materials, while the optical system requires all structures to be black to mitigate stray light. Another example is the sunshade. A sunshade is necessary for the optical interferometer to exclude stray light and for thermal protection. However, for the RF sensor, the sunshade is the primary source of multipath. RF interference (RFI) with spacecraft subsystems is another area of concern. Physical accommodation of all the instruments also has to be coordinated. Overall, a careful system engineering effort is required during mission design.

D. Calibration of the Distributed System

In-orbit calibration of the antenna phase patterns requires analytical and operational coordination with the spacecraft maneuver control and metrology system, e.g., knowledge of relative maneuvers, communications latency, and time synchronization.

E. Acquisition of the Spacecraft Formation

Immediately after launch, the two spacecraft rotate into the sunshaded orientation. After that, the AFF sensor needs to acquire the signals transmitted from the other spacecraft within a reasonable time in concert with the geometrical acquisition of the formation-flying system.

F. Operation of the Distributed System

Given the fact that the sensor is distributed across multiple spacecraft, the following issues need to be addressed carefully: time synchronization, independent reference frequency bases that may drift over time, multiple frequency schemes, inter-spacecraft communication, fault protection, and recovery from partial failures in the multiple-spacecraft formation.

V. Technology Development and Results

In order to assess the feasibility of the AFF sensor for StarLight formation flying, leading technology risk items were investigated. A prototype AFF sensor was developed and evaluated as follows. The RF antenna performance was addressed in the antenna test beds. The sensor scheme and the algorithm performance were tested in the AFF sensor prototype test bed. The end-to-end functionality test was performed outdoors across a 358-meter range. A comprehensive error-budget analysis was performed for the overall performance of the AFF sensor. The results from the test beds were evaluated relative to the error-budget allocations, and the overall performance of the sensor was inferred from the comprehensive error budget populated by the test-bed results. In this manner it has been shown that the AFF sensor will meet the (2-cm, 1-arcmin) 1-σ accuracy in range and bearing-angle estimates within the StarLight mission.

The leading technical concerns addressed were

(1) RF antenna performance within the spacecraft structure—evaluated in the antenna test beds.
    (a) Isolation between transmitting and receiving antennas on the same spacecraft.
    (b) Antenna pattern degradation due to multipath.
(2) Basic algorithms and calibration schemes in a multiple-spacecraft environment (with separate frequency references on each spacecraft)—evaluated in the prototype test bed.
    (a) Basic signal processing algorithms.
    (b) Continuous self-calibration algorithm.
    (c) Algorithm for carrier-aided smoothing of the range observable.
    (d) Asynchronous TDD scheme.
    (e) End-to-end complex Ka-band scheme.
    (f) Temperature calibration.
(3) End-to-end functionality—verified outdoors across a 358-meter range.

Through these tests, the technical concerns have been resolved and retired. The descriptions of the test beds, the results, and a summary of the technology assessment are presented below.

A. RF Antenna Performance—Evaluated in the Antenna Test Beds

The performance of the Ka-band antennas within the StarLight spacecraft structural environment was evaluated in the following antenna test beds. The antennas were prototyped, and physical models of the antenna mounting plate and the spacecraft sunshades (for both the combiner and the collector spacecraft) were constructed. Then the performance of each antenna was assessed within the structurally modeled environment.

1. Isolation between Transmitting and Receiving Antennas. To evaluate the isolation between the transmitting and receiving antennas on the same spacecraft, the antennas and the structural model of the mounting plate were set up as shown in Fig. 2. The transmitting antenna and the adjacent receiving antennas were pointed towards the sky. While the transmitting antenna transmitted, the signals received at the receiving antennas were measured. Isolation of each receiving antenna was defined as the ratio of the received signal power to the transmitted power. Isolation was measured with and without the sunshade models attached. The results are significant:

(1) The measured isolation matches exactly the space loss predicted by Friis' equation. This is an important positive result that shows that there are no significant surface effects on the mounting plate. This result is further supported by the fact that the isolation level remained unchanged when the plate was removed and when multi-layer insulation (MLI) was laid on the plate. Insensitivity to the MLI is desirable because MLI may be used for thermal control.

(2) The isolation between the transmitting and receiving antennas was degraded by the multipath effects from the sunshade. The degradation depended directly upon the shape of the sunshade. Without the sunshade, isolation levels varied in the range of -91 dB to -85 dB. With the combiner sunshade, the range extended from -80 dB to -73 dB. With the collector sunshade, which has the sharper slope away from the antennas, isolation ranged between -86 dB and -80 dB. The sharper the angle of the sunshade away from the antennas, the smaller was the coupling between the antennas.

(3) The repeatability of the isolation levels was poor when the separation between the antennas and the sunshades was varied. This result is due to the fact that the uncertainty in mechanical positioning is comparable to the short wavelength at Ka-band. This fact must be taken into account when considering using the leaked transmitted signal as a part of the self-calibration scheme, as variable biases can be introduced easily by mechanical and thermal variations in the shades, particularly during and after launch.

In a non-TDD, simultaneously transmitting and receiving scheme, the potentially insufficient isolation may lead to self-jamming. The potentially unstable isolation between the transmitting and receiving antennas also may be of concern in using that "leakage" signal for calibration purposes. Depending upon the mission requirements, a TDD scheme with a controllable internal calibration path may be a more attractive alternative.

2. Effect of the Multipath upon the Antenna Pattern. For evaluating the effect of multipath upon the antenna pattern, tests were set up in an anechoic chamber, as shown in Fig. 3. The transmitting and receiving antennas were mounted on the model of the mounting plate, and patterns were cut with and without the sunshade models attached. A pair of patterns, the first without the sunshade and the other with a sunshade, is shown in Fig. 4. From the changes in the power gain pattern shown in this figure, one can infer that the effects of the sunshades on the range and bearing are not negligible.

To evaluate the impact of the antenna pattern deviations on the radio metric performance, the worst-case deviation from a smooth pattern was measured, and its contribution to the error in estimating

Fig. 2. Test setups for the isolation between transmitting and receiving antennas: (a) with no sunshade, (b) with the collector spacecraft sunshade, and (c) with the combiner spacecraft sunshade.

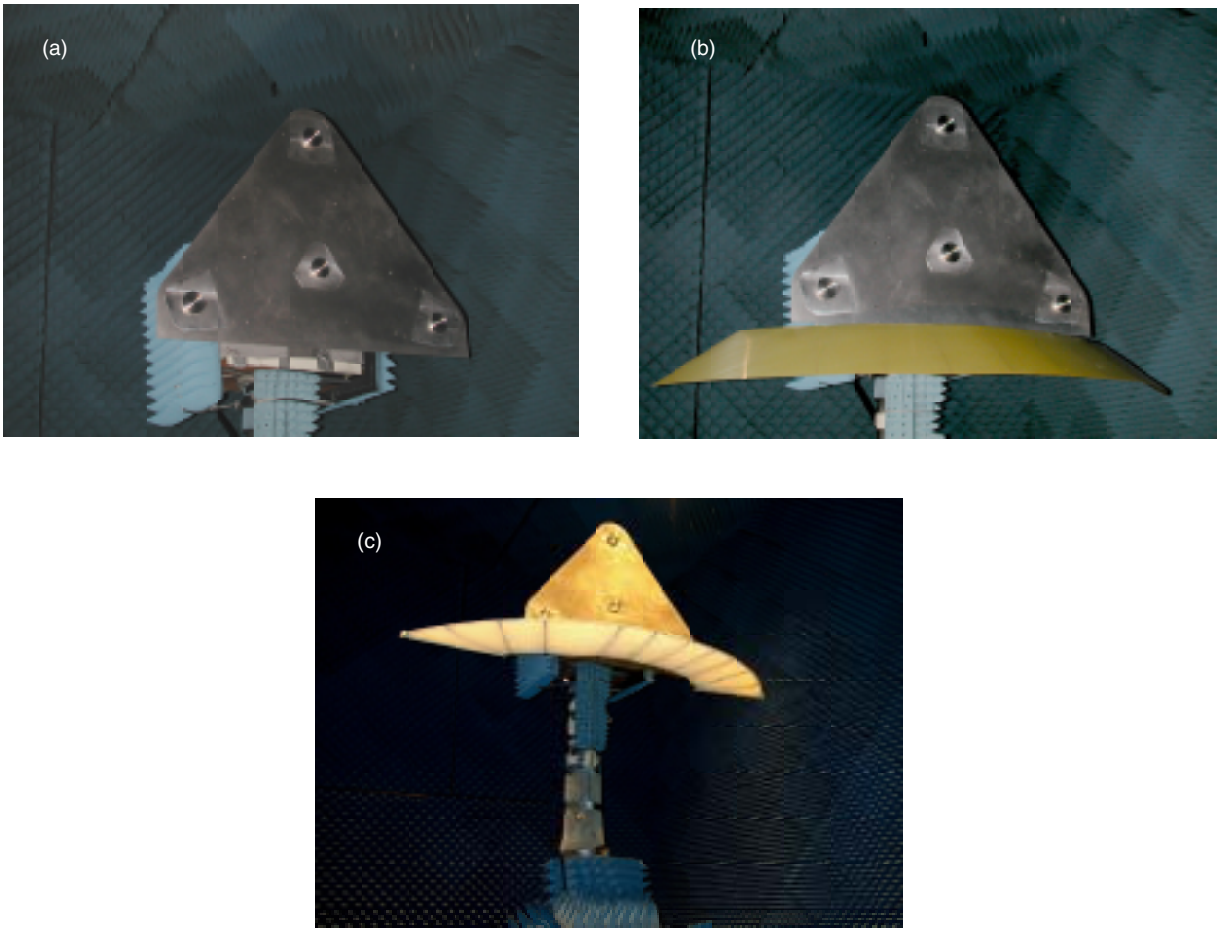

Fig. 3. Test setups for pattern measurements with and without the sunshades: (a) with no sunshade, (b) with the collector sunshade, and (c) with the combiner sunshade.

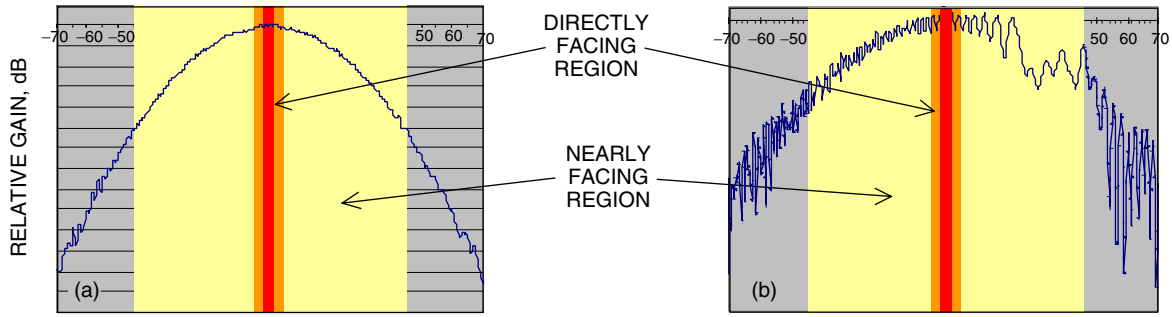

Fig. 4. Antenna gain pattern (a) with no sunshade and (b) with a combiner sunshade.

range and bearing angles was evaluated. Then that error contribution was compared to the error-budget allocation. The results showed that, within the overall error budget, the deviations due to multipath are well within the error allocation. In the "facing" configuration, the sensor can meet the (2-cm, 1-arcmin) requirement in range and bearing-angle estimation. In the "nearly-facing" and "not facing" configurations, the deviations still satisfy the looser requirements for those regions. This result shows that the performance requirements can be met in the StarLight configuration.

B. Basic Algorithms and Calibration Schemes in a Multiple-Spacecraft Environment—Evaluated in the Prototype Test Bed

To verify the basic algorithms and calibration schemes in a multiple-spacecraft environment, a prototype sensor test bed was developed. The test bed is shown in Fig. 5. It is composed of two halves, each side representing a spacecraft. Each half is composed of Ka-band modules and a digital baseband processor. The waveguide attenuators connecting the two halves represent the space loss. The two halves operate with independent frequency references, as they would in orbit. Microwave assemblies are thermally controlled for studies involving thermal sensitivity. This prototype is fully operational. The test results are discussed below.

1. Continuous Self-Calibration Scheme. To continuously and almost instantaneously remove instrumental variations, a continuous self-calibration scheme has been designed. This scheme operates across both spacecraft and calibrates the carrier phase observables and the range observables. This scheme has been verified on the prototype system. Results are shown in Fig. 6. Figures 6(a), 6(b), and 6(c) show the uncalibrated and calibrated phase observables. For this example, after calibration, the residual rate is -3×10^{-9} Hz. Figures 6(d), 6(e), and 6(f) show the uncalibrated and calibrated range observables. In Fig. 6(f), the residual rate is -2.3×10^{-8} chips/s. It is clear from the results that the instrumental variations on the phase and range observables are removed by the calibration technique. The standard deviation of the calibrated observables is within the error-budget allocation.

2. Carrier-Aided Range Estimation. The AFF sensor employs a scheme for smoothing the range observable with the aid of the carrier phase observable. This algorithm is also successfully used in the GPS. However, it is novel for the AFF system because, unlike the GPS where the carrier and code are transmitted from the highly stable sources onboard the GPS satellites, the AFF system generates its own transmitted signals. For that reason the stability of the transmitting and receiving Ka-band modules and the frequency and timing scheme have to be assessed with respect to the feasibility of this algorithm. The

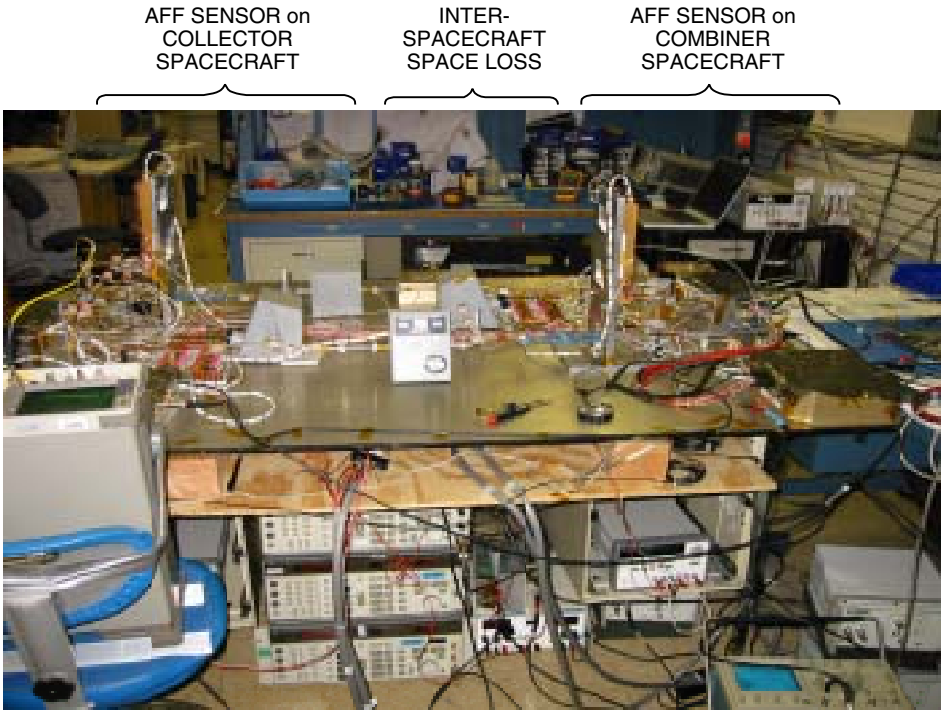

Fig. 5. The AFF prototype system test bed.

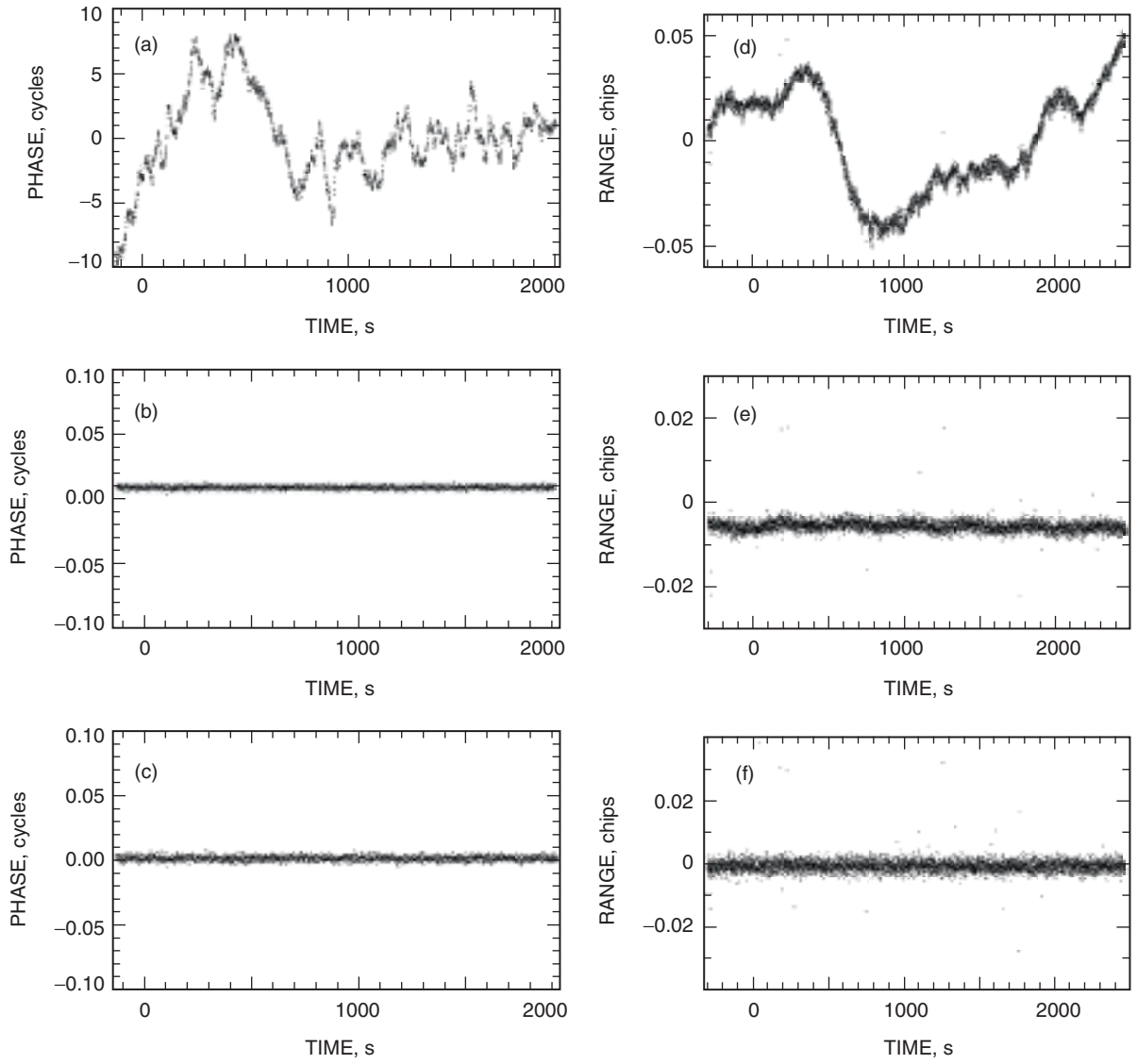

Fig. 6. Continuous calibration results: (a) single-channel phase measurement, (b) differenced phase observable, (c) calibrated phase observable, (d) single-channel range measurement, (e) summed range observable, and (f) calibrated summed range observable.

results in Fig. 7 show that the current AFF sensor design can indeed support this algorithm. Figure 7(a) shows the range observable before carrier-aided smoothing, and Fig. 7(b) shows the observable after 100 seconds of smoothing. The standard deviation of the 1-second ranges is reduced by the expected ratio, about $1/\sqrt{100}$.

3. Asynchronous Time-Division Duplexing (TDD). An asynchronous version of the time-division duplexing scheme that does not require the two spacecraft to synchronize has been verified on the prototype. Both halves of the AFF sensor prototype acquired and maintained lock, and the observed reduction in the signal-to-noise ratio due to duplexing matched predictions.

4. Ka-Band Frequency Scheme. The successful prototype test results confirm that the Ka-band frequency scheme selected for StarLight will work.

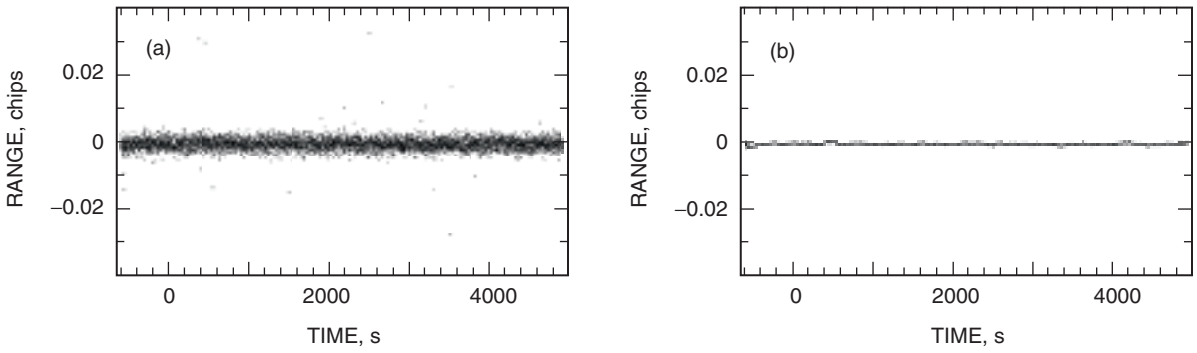

Fig. 7. Results of carrier-aided smoothing on range observables: (a) range observable before carrier-aided smoothing and (b) range observable after 100 seconds of smoothing.

C. End-To-End Functionality Test of the AFF Sensor

An end-to-end radiating test has been performed to verify the end-to-end functionality of the sensor. The two halves of the sensor were positioned 358 meters apart across a valley behind JPL. Both sides transmitted and received at Ka-band. Each side successfully received and tracked both the remote signal and the local self-calibration signal. The phase and the range observables were successfully extracted. One end of the test setup is shown in Fig. 8.

D. Summary of the Technology Results

Three kinds of tests have been performed to evaluate the AFF sensor design. The antenna test beds (Figs. 2 and 3) were used to verify the RF antenna performance within a mock-up of the spacecraft structure environment, and the AFF sensor prototype test bed (Fig. 5) was used to verify the sensor scheme and the algorithm performance. The end-to-end functionality test across a 358-meter range demonstrated the operation of the sensor with signals transmitted through space. The results show that the sensor will work with the required performance of (2-cm, 1-arcmin) 1-σ accuracy in range and bearing-angle estimates within the StarLight mission.

The following leading basic technical concerns have been addressed and are retired at this time:

(1) Algorithms for self-calibration.

(2) Algorithms for carrier-aided smoothing of the range observable.

(3) Antenna pattern degradation due to multipath.

(4) Verification of the complex Ka-band scheme.

Investigation of the isolation between the transmitting and receiving antennas on each spacecraft in the StarLight configuration showed that potentially insufficient and unstable isolation makes a TDD scheme with a controllable internal calibration path a more attractive alternative. This approach has been validated in the AFF prototype test bed. Whether or not TDD is required will need to be determined for different missions on an individual basis.

VI. Associated StarLight Design

A. Spacecraft Accommodation

For the StarLight mission, the spacecraft design team positioned the AFF sensor antennas as far forward as possible, but still behind the sunshade, as shown in Fig. 9. Figure 9(a) shows the accommodation on the combiner spacecraft, and Fig. 9(b) shows the accommodation on the collector spacecraft. Ideally,

Fig. 8. The AFF sensor radiated test for end-to-end functional verification.

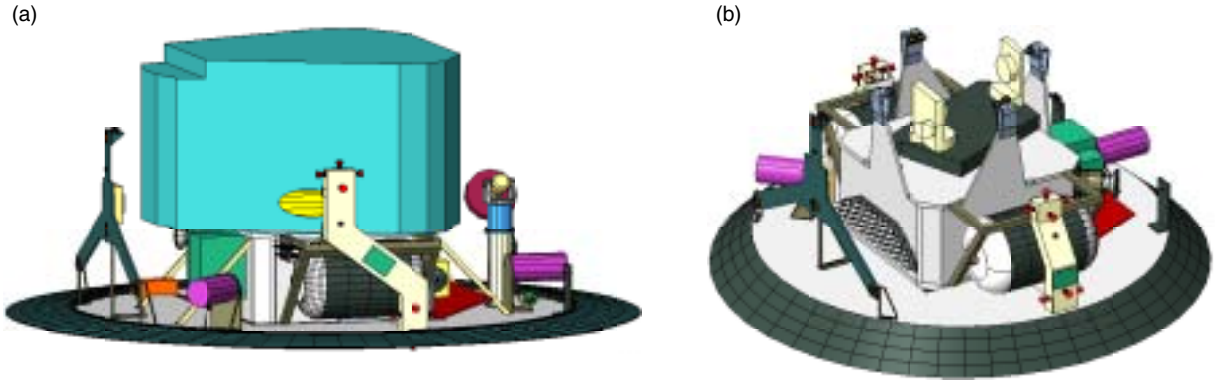

Fig. 9. The AFF sensor accommodation on the (a) combiner spacecraft and (b) collector spacecraft.

the antennas should be mounted at or beyond the outer edge of the sunshades with no structures within view of the antennas. Figure 9 represents the compromise reached for StarLight.

The antenna patterns will need to be measured in the presence of the final sunshade design. Selection of the sunshade material and geometry had not been completed. Simultaneous satisfaction of the optical, RF, and thermal requirements on the shades is a substantial technology challenge.

B. Acquisition of Spacecraft Formation

To minimize the acquisition time, the formation-flying system requires the widest field of view possible from the RF sensor. However, a large field of view exacerbates multipath, which degrades sensor performance and thereby affects the design of the spacecraft and the formation-flying control system, as well as the time (and fuel) needed to reach the observing configuration after acquisition. Trading off all these considerations to optimize performance in some global sense is therefore a complex undertaking.

Currently, an antenna that provides adequate gain to 70 deg off boresight has been designed and assessed for RF performance. Further iterations of field of view versus performance will be required in the mission design stage.

C. Synchronization of the Distributed System

The distributed nature of the sensor on the two spacecraft poses challenges in terms of time synchronization, fault-protection, and recovery from temporary failure on one or both sides. Given that the sensor supports an optical interferometer, the design demands maximum robustness and minimum maintenance. Further work is required in this area.

VII. Conclusion

At this time, the prototype AFF sensor has been extensively evaluated. The leading technical challenges have been addressed through development of a prototype system and tests in multiple test beds to evaluate performance and to verify end-to-end functionality. The results show that the sensor will work with the required performance of (2-cm, 1-arcmin) 1-σ accuracy in range and bearing-angle estimates within the StarLight mission.

These results are directly applicable to the TPF mission. For TPF and any other precision formation-flying missions, it is emphasized that the sensor performance needs to be optimized through design trade-offs involving the sensor, the spacecraft, and the optical interferometer (or any other science instruments). For the precision formation-flying system, performance must be optimized by trading off sensor performance, sensor field of view, spacecraft maneuvers, and formation control design.

VIII. Further Work

The AFF sensor will be further assessed for integration into the TPF precision formation-flying system. In particular, the following technical assessments need to be made for the TPF spacecraft configuration: multipath effects; acquisition techniques; calibration techniques; hand off to a finer sensor with a narrower field of view; locations of the antennas; and trade-offs involving sensor performance, field of view, formation-flying control design, spacecraft design, and interferometer design.

Another area of future work is the investigation of technologies to integrate high-bandwidth inter-spacecraft communication with the AFF sensor. This concept is motivated by the fact that the sensor already provides an inter-spacecraft link with the highest performance in the facing configuration, and the interferometer requires the highest data bandwidth in the facing configuration to support high-speed control loops for the siderostats. Therefore, the RF link may be exploited.

Acknowledgments

The authors would like to acknowledge Mike Weiss, Dean Paschen, and Andy Jarski of Ball Aerospace and Technologies Corporation, Boulder, Colorado, for their contribution in the AFF sensor technology activities. They and others at Ball participated in the design team to integrate the AFF sensor to work within the two-spacecraft mission. They also provided the designs for the spacecraft structural models and suggested an asynchronous version of the TDD scheme that is applicable to StarLight and other future missions.

The authors would also like to acknowledge Andrew M. Vozoff of the Jet Propulsion Laboratory for his significant contribution to the antenna isolation tests, Phil Mayers for his enthusiasm and dedication in getting the prototype built, and Thomas Osborne for his significant role in making the measurements for the antenna evaluation.

References

[1] G. Purcell, D. Kuang, S. Lichten, S.-C. Wu, and L. Young, "Autonomous Formation Flyer (AFF) Sensor Technology Development," Paper 98-062, 21st Annual AAS Guidance and Control Conference, Breckenridge, Colorado, February 4–8, 1998.

[2] G. Purcell, D. Kuang, S. Lichten, S.-C. Wu, and L. Young, "Autonomous Formation Flyer (AFF) Sensor Technology Development," *The Telecommunications and Mission Operations Progress Report 42-134, April–June 1998,* Jet Propulsion Laboratory, Pasadena, California, pp. 1–21, August 15, 1998. http://tmo.jpl.nasa.gov/tmo/progress_report/42-134/134J.pdf

[3] M. Sue, G. Purcell, M. Ciminera, M. Gudim, and T. Peng, "Frequency Selection for Formation Flying of StarLight, a Deep Space (Category B) Mission," Space Frequency Coordination Group SFCG-21, Cayenne, French Guyana, September 9–18, 2001.

[4] K. Lau, S. Lichten, L. Young, and B. Haines, "An Innovative Deep Space Application of GPS Technology for Formation Flying Spacecraft," American Institute of Aeronautics and Astronautics Paper AIAA 96-3819, *Guidance, Navigation and Control Conference Proceedings*, San Diego, California, July 1996.

[5] G. Blackwood, O. Lay, W. Deininger, M. Gudim, A. Ahmed, R. Duren, C. Noecker, and B. Barden, "StarLight Mission: A Formation Flying Stellar Interferometer," SPIE Conference: Astronomical Telescopes and Instrumentation, Waikoloa, Hawaii, August 22–28, 2002, Kona, Hawaii, August 2002.

[6] J. Tien, G. Purcell, L. Young, M. Aung (Gudim), J. Srinivasan, L. Amaro, E. Archer, A. Vozoff, and Y. Chong, "Technology Validation of the Autonomous Formation Flying Sensor for Precision Formation Flying," to be presented at the IEEE Aerospace Conference, Big Sky, Montana, March 2003.